J. Chem. Sci. Vol. 128, No. 10, October 2016, pp. 1519–1526. © Indian Academy of Sciences. *Special Issue* on CHEMICAL BONDING
DOI 10.1007/s12039-016-1160-7

PERSPECTIVE ARTICLE

Bonding and Reactivity Patterns from Electrostatic Landscapes of Molecules

SHRIDHAR R GADRE[a,b,*] and ANMOL KUMAR[a]

[a]Department of Chemistry, Indian Institute of Technology, Kanpur, Uttar Pradesh 208 016, India
[b]Interdisciplinary School of Scientific Computing, Savitribai Phule Pune University, Pune, Maharashtra 411 007, India
e-mail: gadre@iitk.ac.in

MS received 28 July 2016; revised 11 August 2016; accepted 12 August 2016

Abstract. The topographical analysis of molecular electron density (MED) and molecular electrostatic potential (MESP) offers insights into the bonding and reactivity patterns through the critical points (CPs) of these scalar fields. The MESP is found to be particularly useful for describing sites of electrophilic attack and weak intermolecular interactions. MESP is also shown to clearly distinguish between the lone pairs and π-delocalization. The concept of atoms in molecules (AIM) which has so far been primarily based on the gradients of MED, has recently been extended *via* the use of MESP. The portrayal of AIM through MESP clearly reveals the electron rich atoms in the molecule and also provides the details of the preferred direction of approach of an electrophile. This perspective briefly summarizes the prominent features of MESP topography and provides a future outlook.

Keywords. Molecular electrostatic potential; molecular electron density; critical points; lone pairs; atoms-inmolecules.

1. Preamble

A molecular system comprising of N electrons is described by its wave function, dependent on 3N spatial co-ordinates apart from the spin variables. The difficulties in even listing out such a wave function as a function of 3N spatial co-ordinates numerically were highlighted[1] by Hartree's historical remark that 'if we were to print the wave function values for the ground state of the iron atom with sufficiently small intervals in all the electronic coordinates, we should require a whole library to house the books in which they were printed'. There are much larger practical difficulties involved in the tabulation and analysis of the wave function of a large molecular system. However, as succinctly put by Coulson,[2] the aim of a theoretical chemist is to obtain 'primitive patterns of understanding' offered by such a complicated, multi-dimensional wave function and not to get lost in the 'horde of numbers gushing out of a computer'. With the advents in computational hardware and software, the computation of accurate molecular wave function has become practically feasible in the last few decades. Due to this, the need for developing interpretative tools is felt even more acutely. Quantum chemists have engaged themselves in developing such methods for the analysis of complicated molecular wave functions. Here are some examples.

(i) The charge density bond order matrix[3] in the Hückel theory
(ii) Population analysis developed by Mulliken[4]
(iii) The frontier orbitals introduced by Fukui[5]
(iv) Density matrices and natural orbitals systematically developed and popularised by Löwdin.[6]

2. Molecular Electron Density (MED) and its Topography

The development of density functional theory (DFT) by Hohenberg and Kohn[7] introduced a revolutionary idea of employing the three-dimensional electron density $\rho(\mathbf{r})$, as a basic variable, in place of the multi-dimensional wave function $\psi(\mathbf{x}_1, \mathbf{x}_2, \ldots\ldots \mathbf{x}_N)$. Here $\mathbf{x}_i$ denotes the combined space-spin co-ordinates of the electron i, with N being the number of electrons. Within DFT, the properties of the ground state of a many-electron system emerge as functionals of the corresponding electron density, $\rho(\mathbf{r})$. The three-dimensional scalar field of the molecular electron density (MED), $\rho(\mathbf{r})$, thus assumes a fundamental role. The entire

*For correspondence
Celebrating 100 years of Lewis Chemical Bond

edifice of density functional theory (DFT) was erected on the basis of the theorems of Hohenberg and Kohn,[7] followed up by the work of Kohn and Sham.[8] Several energy density functionals have become available[9–12] in the last 30 years or so for accurately describing the electronic structure of atoms and molecules. The search for the elusive Hohenberg-Kohn functional is still continuing, with a hope that highly accurate practical computation of the electronic structure of atoms and molecules would be feasible in the near future.

Methods for the interpretation of the features of MED, such as chemical bonds, lone pairs, π delocalisation *etc.*, were pioneered[13–15] by Bader and co-workers. This work culminated into a treatise, *viz., Atoms in Molecules: A Quantum Theory* by Bader.[16] The MED, $\rho(\mathbf{r})$, extracted for a many electron wave function $\psi(\mathbf{x}_1, \mathbf{x}_2, \ldots\ldots \mathbf{x}_N)$ is defined by the equation

$$\rho(\mathbf{r}) = N \sum_{\sigma} \int |\Psi(\mathbf{x}_1, \mathbf{x}_2, ..., \mathbf{x}_N)|^2 \, d^3r_2 ... d^3r_N \Big|_{\mathbf{x}_1 = \mathbf{x}} \tag{1}$$

Here, $\mathbf{x}_i$ stands for combined space-spin co-ordinates of the electron i, N is the number of electrons and Σ denotes the summation over the spin co-ordinates of all the electrons. The basic bonding features of a molecule were brought out by Bader[13–16] in terms of the critical points (CP) of the corresponding MED. A critical point (CP) of a function $f(x_1, \cdots x_n)$ is defined as a point, P, where for $i = 1$ to n,

$$\nabla_i f(x_1, x_2, \ldots, x_n)|_P = \left.\frac{\partial f}{\partial x_i}\right|_P = 0 \tag{2}$$

A further characterisation of the CP at the point P is done by inspecting the nature of the eigenvalues of the corresponding Hessian matrix, H_{ij} where

$$H_{ij} = \left[\frac{\partial^2 f}{\partial x_i \partial x_j}\right]_P \tag{3}$$

The rank of a CP is the number of non-zero eigenvalues. Thus, for the three-dimensional scalar field of MED, the maximum rank equals 3. A CP is said to be degenerate if at least one of the eigenvalues is equal to 0. Thus, for a nondegenerate CP, the rank, R equals 3. The signs of the eigenvalues determine the signature of the CP, for instance for a nondegenerate CP that corresponds to a maximum, all the eigenvalues are negative. Thus such a CP is labelled as (3, −3). In general, a CP is labelled as (R, σ), where σ, the signature stands for the excess number of positive eigenvalues over the negative ones. A nondegenerate minimum carries a label of (3, +3). If some of the eigenvalues are positive and the others are negative, such a CP is termed as a saddle point. There are two types of nondegenerate saddle points for a 3-dimensional scalar field such as MED, *viz.*, (3, +1) and (3, −1). For a lucid introduction to this subject, see the book by Bader[16] and a monograph by Gadre and Shirsat[17] as well as a semi-popular article by Stewart.[18] Bader and co-workers have carried out extensive topographical investigations[13–16] on MED since 1970. The highlights of Bader's atoms-in-molecules (AIM) studies can be briefly summarized as follows.

(i) A pair of bonded atoms of a molecule always exhibits a (3, −1) saddle point between them. Such a saddle point was called by Bader as a bond critical point (BCP). A unique gradient path traversing through BCP connecting the two bonded atoms is termed as the "Atomic Interaction Line" (AIL) or "Bond Path" in the AIM picture. A network of such AILs of the whole molecule is known as the molecular graph.

(ii) A ring structure in a molecule shows up as a (3, +1) saddle point, called as a ring saddle point (RCP).

(iii) A cage structure appears as a (3, +3) cage critical point (CCP), *viz.,* a minimum in MED.

(iv) The MED exhibits maxima at the nuclear sites. However, there are some molecules exhibiting non-nuclear maxima.[16,19] Such maxima are shown by Li_2, C_2, Na_4, *etc.*

(v) Bader found that the value of MED, ρ_b at a bond saddle point may be used to define the order n, of the corresponding bond by the relation

$$n = \exp[A(\rho_b - B)] \tag{4}$$

where A and B are fitting parameters. The eigenvalues of the Hessian matrix at the BCP can be used to define the bond strain, bond ellipticity, *etc*.[16]

(vi) Most fundamentally, AIM defines the existence of atoms in a molecule based on the properties of gradient of MED. An atom in the molecule is defined by a region of molecular space which is limited by zero flux surface of gradient of MED, which obeys the Equation $\nabla\rho(\mathbf{r}).d\mathbf{S} = 0$. Such a region of molecular space is called the atomic basin. The set of gradient paths of MED originating in an atomic basin terminates at the enclosed nucleus.[16] However, as the zero flux surface of $\nabla\rho(\mathbf{r})$ does not enclose an atom completely, Bader suggested use of low valued-isosurface of MED for limiting the size of atomic basins.

Some of the features of MED topography are illustrated below in Figure 1 with the examples of three molecules, *viz.,* methanol, cycopropane and cubane.

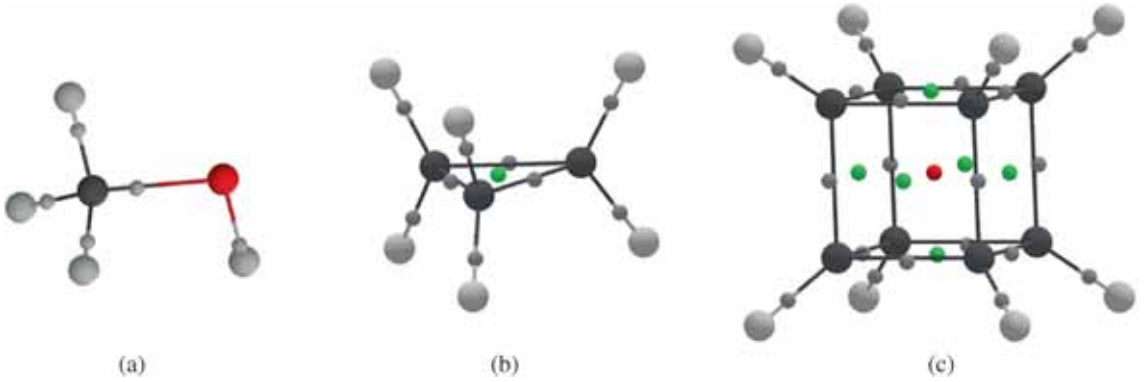

Figure 1. Critical points (CPs) of the electron density for **(a)** CH_3OH, **(b)** C_3H_6 and **(c)** C_8H_8 molecules. The grey, green and red dots denote (3,−1), (3,+1) and (3,+3) CPs. See text for details.

The MED and molecular electrostatic potential (MESP) values for all the illustrations in this perspective are computed using the Gaussian09 suite of programs[20] and DAMQT package,[21] employing MP2/6-31+G(d) level geometry optimization and property evaluation. Figure 1(**a**) shows all the bonded atom pairs in the methanol molecule connected with a (3, −1) CP (BCP) each. Apart from such BCP's, the cyclopropane molecule (*cf.* Figure 1(**b**)) is seen to display a (3, +1) CP (RCP) in its MED topography. A (3, +3) cage CP (CCP) in MED is a signature of a topographical cage as may be noticed for the case of the cubane molecule displayed in Figure 1(**c**). Several years ago, it was noted[22a,b] that the bond paths for strained molecules such as cyclopropane are bent outwards w. r. t. the straight lines joining the ring carbon atoms, in agreement with the 'bent banana bonds' proposed by Coulson and Moffitt.[22c] The MED bond CP's of the cubane molecule are also seen to lie outwards w. r. t. the straight lines joining the carbon atoms (cf. Figure 1(c)).

As summarized in (iv) above, non-nuclear maxima in MED have been observed[16,19] in Li and Na clusters. Figure 2 shows non-nuclear maxima in Li_2 and Na_4 clusters. Contours of MED are projected in the planes containing the atoms of these clusters to bring out their unusual pattern. The two bond CPs can be observed between the two Li atoms in the Li_2 molecule (*cf.* Figure 2(**a**)) *i.e.* the atoms are not bonded directly, but rather through a non-nuclear maximum (orange dot). Similarly, six bond CPs can be noticed in Na_4 cluster (*cf.* Figure 2(**b**)) containing two non-nuclear maxima. A heuristic explanation for the case of Li_2 has been offered by Edgecombe *et al.*,[19c] in terms of the Li atoms retaining much of their atomic character during the molecule formation.

The above discussion is a very brief summary of the voluminous work done by Bader and his associates. Many further details are provided in Ref. [16]. AIM has become a widely used tool for the analysis of bonding features in molecules as well as crystals. Experimentally measured electron densities have also been subjected to AIM analysis.[23]

It may be pointed out that some other molecular scalar fields have also been investigated in the literature. These include the bare nuclear potential (BNP)[24] and molecular electron momentum density.[25] However, the

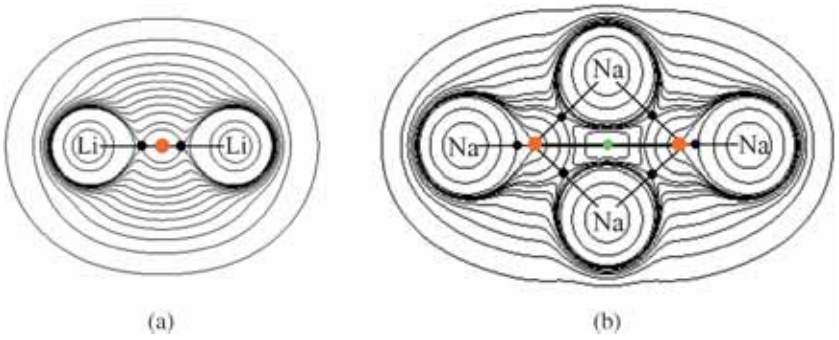

Figure 2. Schematic representation of non-nuclear maxima in molecular electron density along with contours of MED in **(a)** Li_2 and **(b)** Na_4 molecules. See text for details.

scalar field of molecular electrostatic potential (MESP) has been used extensively in the chemical literature for exploring the features of bonding and reactivity in molecules.[17]

3. Molecular Electrostatic Potential (MESP) and its Topography

The MESP, $V(\mathbf{r})$, is defined as

$$V(\mathbf{r}) = \sum_{A}^{N} \frac{Z_A}{|\mathbf{r} - \mathbf{R}_A|} - \int \frac{\rho(\mathbf{r}')\mathrm{d}^3\mathrm{r}'}{|\mathbf{r} - \mathbf{r}'|} \tag{5}$$

where $\{Z_A\}$ are the fixed nuclear charges placed at $\{\mathbf{R}_A\}$ and $\rho(\mathbf{r})$ is the corresponding continuous electron density. Classically, the MESP, V($\mathbf{r}$), at a point $\mathbf{r}$ in space is defined as the work done in bringing a unit test positive test charge from infinity to the reference point $\mathbf{r}$. As seen from Eq. (5), MESP can attain positive (including zero) as well as negative values. MESP is positive in the regions wherein the first term on the r.h.s. of Eq. (5), *viz.*, the nuclear contribution, dominates. On the other hand, MESP becomes negative in the regions where the electronic contribution (the second term on the r.h.s. of Eq. (5)) overrides the nuclear contribution. This as well as other properties of MESP were exploited by the early pioneers[26–28] of molecular electrostatics, *viz.*, the Pullmans, Tomasi and Politzer, for investigating reactivity patterns of molecules, including the sites of electrophilic and nucleophilic attacks. Weinstein *et al.*,[29] proved that the spherically averaged atomic electrostatic potential (ESP) is a monotonically decreasing function of the radial distance, r. In a similar spirit, Sen and Politzer[30] showed that the atomic anions exhibit a negative-valued minimum in the spherically averaged MESP, $V(\mathbf{r})$. They correlated this position of the minimum, r_m with the radius of the atomic anion.

Gadre and co-workers derived a generalisation of both of these results to molecular systems.[31a,b] Their first result states that the electrostatic potential of any molecule cannot show a non-nuclear maximum at any point in space. The proof of this theorem is quite straightforward and hinges upon the Poisson equation and non-negativity of the corresponding electron density $\rho(\mathbf{r})$. The second result due to Pathak and Gadre deals with the MESP of molecular anions,[31b] wherein it was shown that every molecular anion is surrounded by a sheath of negative potential on all the sides. In particular, there exists a minimal surface, S enclosing the nuclear framework of the anion, which obeys the equation $\nabla V(\mathbf{r}).\ d\mathbf{S} = 0$. It was shown by them that the integral of $\nabla V(\mathbf{r}).\ d\mathbf{S}$ over the surface, S can be converted to a volume integral over the enclosing volume, Ω by the use of Gauss' theorem. In conjunction with the Poisson equation, it leads to

$$\begin{aligned} \oint_S \nabla V.\ d\mathbf{S} &= \int_\Omega \nabla^2 V d^3r \\ &= 4\pi \int_\Omega \left\{ \rho(\mathbf{r}) - \sum\nolimits_A Z_A \delta(\mathbf{r} - \mathbf{r}_A) \right\} d^3r \\ &= 0 \end{aligned} \tag{6}$$

since $\nabla V(\mathbf{r}).\ d\mathbf{S} = 0$. As a consequence, the net charge on the anion resides outside this minimal surface, S. Gadre and coworkers[32] proposed that this surface could be used for describing the spatial extent, anisotropy and reactivity of molecular anions. In particular, such a minimal surface and the details of the MESP minima were used by them for providing insights on the cation binding to anionic systems.[33,34] This valuable information of cation binding sites is obtained more directly by mapping the locations of the most negative minima, *viz.,* the (3, +3) CPs of MESP of anions.

The salient topographical features of MESP investigated by Gadre and co-workers are summarized below.

(i) There are no non-nuclear maxima in MESP. This is in contrast with the scalar field of MED, wherein such non-nuclear maxima indeed exist for several molecular systems, as discussed above.

(ii) Similar to the feature shown by MED, a pair of bonded atoms always shows a (3, −1) CP between them.

(iii) Akin to the MED, the (3, +1) and (3, +3) ring and cage CPs, respectively, appear for MESP as well.

(iv) However, in contrast to the MED, the lone pairs and π bonds always show up as negative-valued local minima in MESP.

(v) In addition, there exist (3, +1) saddle points that connect the (3, +3) MESP CPs. Thus in contrast with MED, the existence of a (3, +1) CP in MESP is not always indicative of a ring structure (Figure 3).

(vi) As described above, molecular anions exhibit a minimum in any outward direction from a nuclear site and a neutral minimal surface exists.

(vii) There exists a relation among the number of non-degenerate CPs of a scalar field such as MED or MESP, *viz.,*

$$n_{+3} - n_{+1} + n_{-1} - n_{-3} = n_- - n_{+.} = \chi \tag{7}$$

Here, χ is called the Euler characteristic and n_{+3} denotes the number of (3,+3) CP's and n_- denotes the number of asymptotic maxima, *etc*.

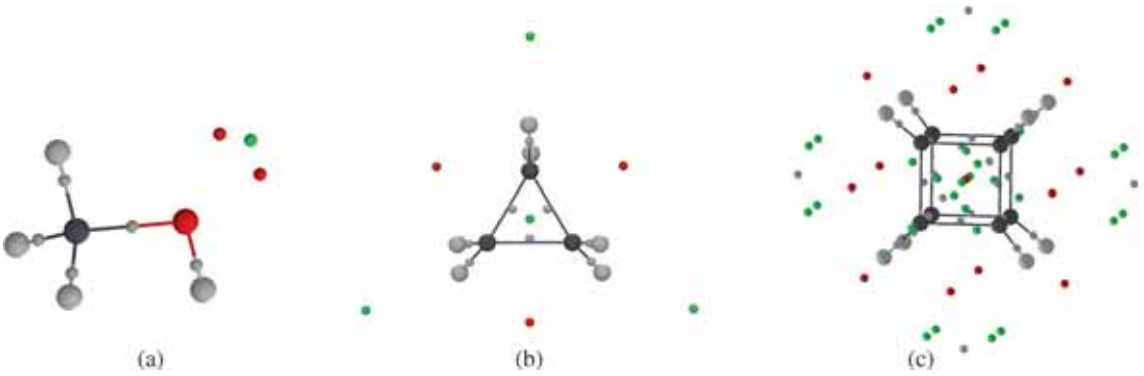

Figure 3. Critical points (CPs) of molecular electrostatic potential for **(a)** cyclopropane (C_3H_6), **(b)** methanol (CH_3OH) and **(c)** cubane (C_8H_8) molecules. The grey, green and red dots denote (3, −1), (3,+1) and (3,+3) CPs, respectively. See text for details.

In this respect also MESP differs from MED. For MED, χ always equals −1 whereas for MESP, the Euler characteristic, χ can attain positive as well as negative values including zero.

(viii) It was pointed out by Lebouf *et al.*,[35] that the Euler characteristic, χ can be determined by texturing the MESP on a sphere of large radius centred at the centre of mass of the molecule. Denoting the number of asymptotic maxima (regions wherein MESP dies to zero negatively) to be n_- and the number of asymptotic minima by n_+, they showed that the Euler characteristic, $\chi = n_- - n_+$. This treatment was later modified by Roy *et al.*,[36] in terms of the corresponding gradient vectors of MESP. A region-wise Poincaré-Hopf (PH) relation was also proposed by them wherein the Euler characteristic, χ is expressed as $\chi = n_o - n_i$. The terms n_o and n_i denote the number of islands showing outflux and influx of $\nabla V(\mathbf{r})$ w.r.t. to the radial vector $\mathbf{r}$ of a finite sized sphere centered at the centre of mass of the molecule. It may be pointed out that the PH relation is only a necessary condition for ensuring the mapping of all the critical points for a given molecular system. It does not offer a sufficient condition for this purpose.

4. Lone Pairs, Lone Pair...π Interactions and reaction mechanism

A recent work[37] by Kumar *et al.,* proposed the definition of a lone pair and suggested a method to distinguish it from π delocalisation. It is noteworthy that such a general definition did not exist in the literature although the term 'lone pair' has been an essential ingredient in any discussion of chemical bonding. Most of the chemists rely on the molecular orbital picture for defining the lone pair. For this purpose, Kumar *et al.*,[37] utilized the topographical characteristics of MESP, noting that lone pairs as well as π-delocalisation exhibit a negative-valued MESP minimum *viz.,* (3, +3) CP.

It was observed by them that the directional nature and sharp variation of MESP are distinctive features of the lone pair vis-à-vis those of π-delocalisation. They proposed the following criterion for identifying a lone pair. The magnitude of the eigenvalue at the (3, +3) CP that corresponds to the lone pair is numerically greater than 0.025 a.u. and the eigenvector associated with it nearly points in the direction (angle $< 5°$) of the atom on which it is localised. This was illustrated by them with the help of several examples. For instance, the 'rabbit ears' (*i.e.,* the lone pairs) of the water molecule have the largest eigenvalue of 0.14 a.u. and the corresponding eigenvector makes an angle of 1.4° with the line joining the MESP minimum with the oxygen nucleus. $CH_3NH\cdot$ radical also shows similar characteristics. However, the CPs denoting π-delocalization in benzene and σ-aromaticity in cyclopropane molecules do not follow the above attributes of lone pair (Figure 4).

It is noteworthy that such a general definition of lone pair is offered in terms of the scalar field of MESP rather than in terms of molecular orbitals. It is known that molecular orbitals are not unique and also are heavily dependent on the basis set used. The scalar fields of MED and MESP do not suffer from this drawback. In particular, the topographical features of MESP have been shown to be only feebly sensitive to the level of theory and basis-set.[38]

The lone pair... π interactions have been extensively investigated in recent years.[39–41] The above definition of lone pairs, in conjunction with the MESP picture of electron-deficient π-systems, offers valuable insights in this type of weak bonding. The prototype electron deficient test systems employed in the literature for studying lone pair... π interactions are hexafluorobenzene, tetracyanobenzene, trinitrobenzene, *etc*. Typical anions

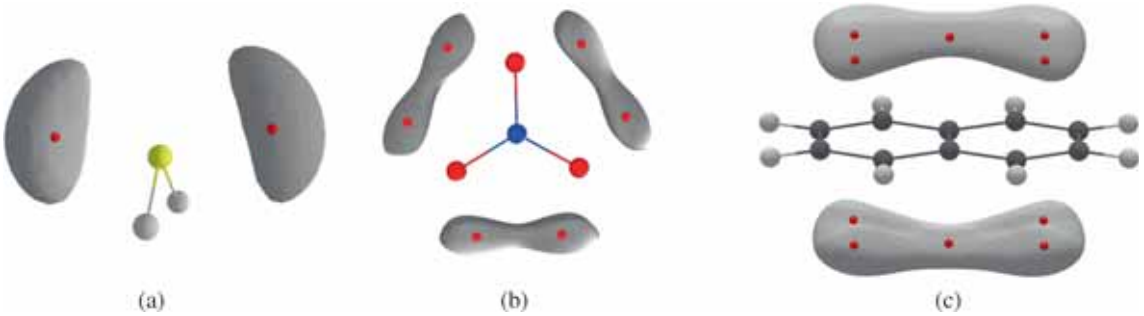

Figure 4. The negative-valued (3,+3) CPs of MESP (red dots) denoting lone pairs and π-cloud in **(a)** hydrogen sulphide (H_2S), **(b)** nitrate (NO_3^-) ion and **(c)** naphthalene ($C_{10}H_8$) molecule, along with the respective grey coloured MESP isosurfaces of values -0.020, -0.24, and -0.021 a.u. The (3,+1) and (3, -1) CPs are not shown for the sake of clarity. See text for details.

employed in these investigations include cyanide, azide, thiocyanide, fluoride, nitrate, *etc*. The lone pairs as well as π-electron clouds in such systems are brought out as (3, +3) CPs of MESP. The corresponding eigenvectors and the associated eigenvalues permit a distinction between these two kinds of electron concentration.

Recent electrostatics-based studies by Mohan *et al.*,[42] and Gadre *et al.*,[43] have brought out the details of these lone pair...π weak bonding interactions. It was found by them that the lone pairs get oriented towards the most positive potential on the van der Waals surface of the electron-deficient π-systems. Further they noticed[42,43] a linear correlation between lone pair...π interaction energy and the MESP minimum value corresponding to the lone pair.

The distinction between the electron localization pattern of lone pair and π charge was exploited earlier by Balanarayan *et al.*,[44] who explored the reaction mechanism of cycloaddition reaction. The reaction paths of two prototype 1,3-dipolar cycloaddition reactions *viz.*, HCNO + HCCH and NNCH + HCCH were probed by them through MESP topography (Figure 5). The picture of electronic shifts brought out by MESP topography offered a direct correspondence with the curved arrows drawn in the organic reaction mechanisms.[45] This study brought out the use of MESP as an effective tool for

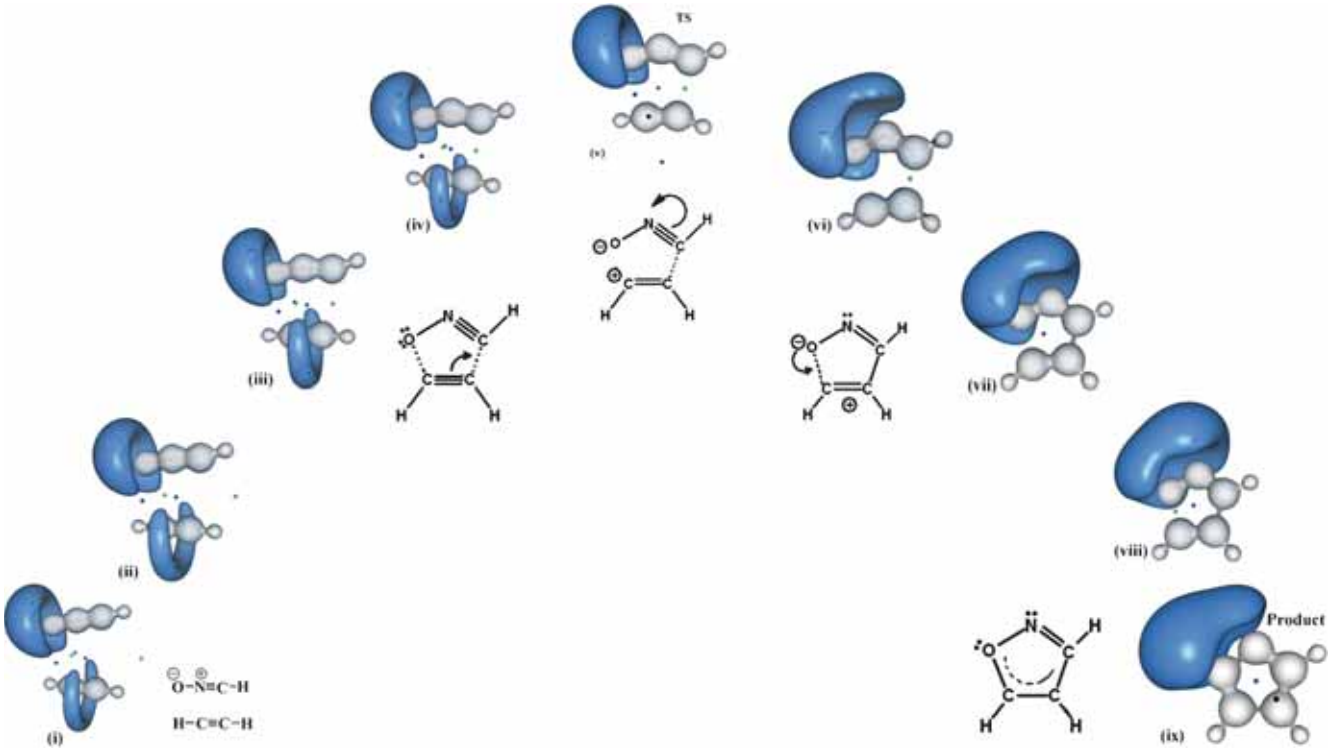

Figure 5. Reaction mechanism of a 1,3-dipolar cycloaddition reaction between HCNO and HCCH as depicted by MESP topography.[44] Blue isosurfaces denote electron-rich regions. See text for details.

understanding the reaction mechanisms and requires detailed follow-up investigations on a variety of organic reactions.

5. MESP-based Gradient Paths and AIM

As discussed above, the MED-based AIM theory developed by Bader and coworkers[16] has gained wide acceptability in the quantum chemistry and molecular physics communities. The recent works by Kumar and Gadre[46,47] have attempted the use of the gradient paths of MESP, *viz.,* $\nabla V(\mathbf{r})$, for developing MESP-based AIM. It may be noted that $-\nabla V(\mathbf{r})$, the negative gradient of MESP is the internal electric field of the molecule generated by the nuclear charges and the continuous electron density distribution. The molecular space is thus partitioned into atomic basins based on the zero flux surfaces (ZFS) of $\nabla V(\mathbf{r})$. Unlike MED-based AIM, MESP-based one shows that the ZFS of $\nabla V(\mathbf{r})$ completely encloses the electron-rich atoms or groups of atoms in the molecule. For instance, the oxygen atom in the CO molecule has a naturally closed MESP-based atomic basin around the oxygen atom. On the other hand, as seen above, MED-based atomic basins of both the atoms in CO are open and only virtually limited by the isosurface of MED in the asymptotic regions. Similarly there is a single closed ZFS of $\nabla V(\mathbf{r})$ around the BF_3 group in the co-ordination complex, NH_3BF_3. Very good qualitative correlation is found for the closed nature of ZFS of $\nabla V(\mathbf{r})$ and the NMR chemical shifts of the corresponding shielded atom/s. An atom possessing a closed ZFS of $\nabla V(\mathbf{r})$ around it shows lower value of chemical shifts in NMR studies indicating shielded nature of that atom. Although much work yet remains to be done, these works dealing with MESP-based AIM open new avenues for exploring reactivity and spectral patterns of molecules.

6. Summary and Future Outlook

The scalar field of molecular electron density (MED) has been extensively explored in the chemical literature for understanding the structure, bonding and reactivity of molecules. Its sister scalar field, *viz.,* molecular electrostatic potential (MESP) has remained relatively less explored for unearthing the above features, although it is directly related to MED through the Poisson equation. As seen above, MESP exhibits rich topographical features and is directly connected with several chemical concepts such as mapping of electrophilic sites,[48] anionic anisotropies,[31] Clar's aromatic sextets,[49a] Hammett constants,[49b] *etc*. The MESP-based AIM recently proposed by the present authors indeed holds promise. It brings out the anisotropy in the gradient paths for the molecule under consideration which could be employed for understanding the stereodynamics of the interacting molecules. It goes beyond the examination of only the scalar features of MESP and, in our opinion, holds enormous potential for understanding the molecular properties and the reactive patterns.

MESP is known to be a valuable tool for predicting directionality of approach of two interacting species. A model named as Electrostatic Potential for Intermolecular Complexation (EPIC) has earlier been proposed and extensively utilized for assembling molecular aggregates.[50] It has been recently generalised into a molecular cluster building algorithm.[51a] This has been successfully used for a step-by-step growth of molecular clusters of benzene, CO_2, *etc*.[51b,c] In our opinion, this approach would be immensely useful for building up large molecular clusters and eventually shed light on the likely atomic contact patterns in molecular crystals.

Acknowledgments

SRG is thankful to the Department of Science & Technology (DST), New Delhi for the award of J C Bose Fellowship. AK thanks the Council of Scientific & Industrial Research (CSIR), New Delhi for the award of a Research Fellowship.

References

1. Hartree D R 1947 *Rep. Prog. Phys.* **11** 143
2. Coulson C A 1960 *Rev. Mod. Phys.* **32** 170
3. Coulson C A 1939 *Proc. Roy. Soc. London* **A169** 413
4. Mulliken R S 1955 *J. Chem. Phys.* **23** 1833
5. Fukui K, Yonezawa T and Shingu H 1952 *J. Chem. Phys.* **20** 722
6. Löwdin P-O 1955 *Phys. Rev.* **97** 1474
7. Hohenberg P and Kohn W 1964 *Phys. Rev.* **136** B864
8. Kohn W and Sham L J 1965 *Phys. Rev.* **140** 1133
9. (a) Becke A D 1988 *Phys. Rev.* **A38** 3098; (b) Becke A D 1993 *J. Chem. Phys.* **98** 5648
10. (a) Lee C, Yang W and Parr R G 1988 *Phys. Rev.* **A37** 785; (b) Parr R G and Yang W 1990 In *Density Functional Theory of Atoms and Molecules* (Oxford University Press: Oxford)
11. (a) Perdew J P 1986 *Phys. Rev.* **B33** 8822; (b) Perdew J P, Chevary J A, Vosko S H, Jackson K A, Pederson M R, Singh D J and Fiolhais C 1992 *Phys. Rev.* **B46** 6671; (c) Perdew J P and Wang Y 1992 *Phys. Rev.* **B45** 13244
12. (a) Zhao Y, Schultz N E and Truhlar D G 2006 *J. Chem. Theory Comput.* **2** 364; (b) Zhao Y and Truhlar D G 2008 *Theor. Chem. Acc.* **120** 215
13. (a) Bader R F W, Beddall P M and Cade P E 1971 *J. Am. Chem. Soc.* **93** 3095; (b) Bader R F W and Beddall P M 1972 *J. Chem. Phys.* **56** 3320

14. (a) Bader R F W, Stephens M E 1975 *J. Am. Chem. Soc.* **97** 7391; (b) Bader R F W, Anderson S G and Duke A J 1979 *J. Am. Chem. Soc.* **101** 1389
15. (a) Bader R F W, Nguyen-Dang T T and Tal Y 1981 *Rep. Prog. Phys.* **44** 894; (b) Bader R F W, MacDougall P J and Lau C D H 1984 *J. Am. Chem. Soc.* **106** 1594; (c) Bader R F W and MacDougall P J 1985 *J. Am. Chem. Soc.* **1985** 6788
16. R F W Bader 1990 In *Atoms in Molecules: A Quantum Theory* (Oxford: Clarendon Press)
17. Gadre S R and Shirsat R N 2000 In *Electrostatics of Atoms and Molecules* (Hyderabad: Universities Press)
18. Stewart I 1991 *Sci. Am.* **264** 123
19. (a) Besnainou S, Roux M, and Daudel R 1955 *C. R. Acad. Sci. Paris* **241** 311; (b) Cao W L, Gatti C, MacDougall P J and Bader R F W 1987 *Chem. Phys. Lett.* **141** 1; (c) Edgecombe K E and Smith V H Jr. 1993 *Z. Naturforsch.* **48a** 127
20. Frisch M J, Trucks G W, Schlegel H B *et al.* Gaussian 09, Revision A.1, Gaussian, Inc., Wallingford CT, 2009
21. Kumar A, Yeole S D, Gadre S R, Lopez R, Rico J F, Ramirez G, Ema I and Zorrilla D 2015 *J. Comput. Chem.* **36** 2350
22. (a) Bader R F W, Slee T S, Cremer D and Kraka E 1983 *J. Am. Chem. Soc.* **105** 5061; (b) Cremer D and Gauss J 1986 *J. Am. Chem. Soc.* **108** 7467; (c) Coulson C A and Moffitt W E 1947 *J. Chem. Phys.* **15** 147
23. (a) Guillot R, Muzet N, Dahaoui S, Lecomte C and Jelsch C 2001 *Acta Cryst.* **B57** 567; (b) Kubicki M, Borowiak T, Dutkiewicz G, Souhassou M, Jelsch C and Lecomte C 2002 *J. Phys. Chem.* **B106** 3706; (c) Mata I, Molins E, Alkorta I and Espinosa E 2007 *J. Phys. Chem.* **A111** 6425; (d) Mata I, Molins E and Espinosa E 2007 *J. Phys. Chem.* **A111** 9859; (e) Arputharaj D S, Hathwar V R, Guru Row T N and Kumaradhas P 2012 *Cryst. Growth Des.* **12** 4357; (f) Porcher F F, Souhassou M and Lecomte C E P 2014 *Phys. Chem. Chem. Phys.* **16** 12228
24. (a) Tal Y, Bader R F W and Erkku J 1908 *Phys. Rev.* **A 21** 1; (b) Parr R G and Berk A 1981 In *Molecular Electrostatic Potentials in Chemistry and Biochemistry* P Politzer and D G Truhlar (Eds.) (New York: Plenum); (c) Gadre S R and Bendale R D 1986 *Chem. Phys. Lett.* **130** 515
25. (a) Gadre S R and Pathak R K 1981 *Phys. Rev.* **A 24** 2906; (b) Kulkarni S A, Gadre S R, Pathak R K 1992 *Phys. Rev.* **A 42** 4399; (c) Gadre S R, Limaye A C and Kulkarni S A 1991 *J. Chem. Phys.* **94** 8040; (d) Balanarayan P and Gadre S R 2006 *J. Am. Chem. Soc.* **128** 10702
26. (a) Scrocco E and Tomasi J 1975 In *Advances in Quantum Chemistry* Vol. 11 P-O Löwdin (Ed.) (New York: Academic); (b) Tomasi J, Bonaccorsi R and Cammi R 1990 In *Theoretical Models of Chemical Bonding* Vol. 3 Maksič Z B (Ed.) (New York: Springer)
27. (a) Giessner-Prettre C and Pullman A 1972 *Theor. Chim. Acta (Berl.)* **25** 83; (b) Pullman B 1980 *Int. J. Quantum Chem. Quantum Biol. Symp.* P-O Löwdin (Ed.) (New York: Academic) **17** 81
28. (a) Politzer P, Donnelly R A and Daiker K C 1973 *J. Chem. Soc. Chem. Comm.* 617; (b) Politzer P and Weinstein H 1975 *Tetrahedron* **31** 915
29. Weinstein H, Politzer P and Srebrenik S 1975 *Theoret. Chim. Acta (Berl.)* **381** 59
30. Sen K D and Politzer P 1989 *J. Chem. Phys.* **90** 4370
31. (a) Gadre S R and Pathak R K 1990 *Proc. Ind. Acad. Sci. (Chem. Sci.)* **102** 189; (b) Pathak R K and Gadre S R 1990 *J. Chem. Phys.* **93** 1770
32. (a) Gadre S R and Shrivastava I H 1991 *J. Chem. Phys.* **94** 4384; (b) Gadre S R, Kölmel C C, Ehrig M and Ahlrichs R 1993 *Z. Naturforsch.* **A48** 137; (c) Gadre S R, Kölmel C and Shrivastava I H 1992 *Inorg. Chem.* **31** 2279; (d) Luque F J, Orozco M, Bhadane P K and Gadre S R 1994 *J. Chem. Phys.* **100** 6718
33. (a) Gejji S P, Bartolotti L J, Suresh C H and Gadre S R 1997 *J. Phys. Chem.* **B 101** 5678; (b) Gejji S P, Suresh C H, Babu K and Gadre S R 1999 *J. Phys. Chem.* **A 103** 7474
34. Suresh C H, Gadre S R and Gejji S P 1998 *Theor. Chem. Acc.* **99** 151; (b) Gejji S P, Gadre S R and Barge V J 2001 *Chem. Phys. Lett.* **344** 527
35. Leboeuf M, Köster A M, Jug K and Salahub D R 1999 *J. Chem. Phys.* **111** 4893
36. Roy D K, Balanarayan P and Gadre S R 2008 *J. Chem. Phys.* **129** 174103
37. Kumar A, Gadre S R, Mohan N and Suresh C H 2014 *J. Phys. Chem.* **A118** 526
38. Gadre S R, Kulkarni S A, Suresh C H and Shrivastava I H 1995 *Chem. Phys. Lett.* **239** 273
39. Alkorta I, Rozas I and Elguero J 1997 *J. Org. Chem.* **62** 4687
40. Kim D, Tarakeshwar P and Kim K S 2004 *J. Phys. Chem. A* **108** 1250
41. De Hoog P, Gamez P, Mutikainen I, Turpeinen U and Reedijk J 2004 *Angew. Chem. Int. Ed.* **43** 5815
42. Mohan N, Suresh C H, Kumar A and Gadre S R 2014 *Phys. Chem. Chem. Phys.* **42** 18401
43. Gadre S R and Kumar A 2015 In *Noncovalent Forces* S Scheiner (Ed.) (Springer: Heidelberg) p. 391
44. Balanarayan P, Kavathekar R and Gadre S R 2007 *J. Phys. Chem. A* **111** 2733
45. Kermack W O and Robinson R 1922 *J. Chem. Soc. Trans.* **121** 427
46. Kumar A and Gadre S R 2016 *J. Chem. Theory Comput.* **12** 1705
47. Kumar A and Gadre S R 2016 *Aust. J. Chem.* doi: 10.1071/CH16226
48. (a) Mehta G, Gunasekaran G, Gadre S R, Shirsat R N, Ganguly B and Chandrasekhar J 1994 *J. Org. Chem.* **59** 1953; (b) Mehta G, Khan F A, Gadre S R, Shirsat R N, Ganguly B and Chandrasekhar J 1994 *Angew. Chem. Int. Ed.* **33** 1390; (c) Gadre S R and Bhadane P K 1997 *J. Chem. Phys.* **107** 5625
49. (a) Suresh C H and Gadre S R 1999 *J. Org. Chem.* **64** 2505; (b) Suresh C H and Gadre S R 1999 *J. Am. Chem. Soc.* **120** 7049
50. (a) Gadre S R and Pundlik S S 1997 *J. Phys. Chem. B* **101** 3298; (b) Pundlik S S and Gadre S R 1997 *J. Phys. Chem. B* **101** 9657
51. (a) Yeole S D and Gadre S R 2011 *J. Chem. Phys.* **134** 084111; (b) Mahadevi A S, Rahalkar A P, Gadre S R and Sastry G N 2010 *J. Chem. Phys.* **133** 164308; (c) Jovan Jose K V and Gadre S R 2009 *Int. J. Quantum Chem.* **109** 2238